Intracellular Translocation of Iodine-125–Labeled Insulin: Direct Demonstration in Isolated Hepatocytes

Abstract. *Insulin labeled with iodine-125 binds to receptors on isolated rat hepatocytes. At low temperatures initial binding is restricted to the plasma membrane as detected by direct quantitative autoradiographic analysis with the electron microscope. With increasing time and temperature of incubation there is a systematic and progressive translocation of autoradiographic grains to a highly limited area of the cell periphery representing no more than 15 percent of the radius of the cell.*

The mechanism by which insulin produces its diverse effects on cells is complex and poorly understood. Binding to a cell surface receptor is the initial step and the hormone receptor complex, in some way, generates a subsequent series of reactions that lead to a biological response (*1*). It has been suggested that the hormone receptor complex may be directly linked to a possibly intracellular degradative pathway in liver (*2*). This degradative pathway might in turn be a mechanism for either terminating or generating an intracellular signal. Further, it has been shown that the binding of insulin to the cell is associated with changes in both the affinity and concentration of the insulin receptor (*3*). Whether these or other steps in insulin action subsequent to binding are related to the hormone, the receptor, or to a product of the interaction is unknown. Whereas the hormone receptor interaction has been studied extensively by a direct binding technique with iodine-125–labeled insulin, there is little information on the fate or role of insulin following receptor binding. We have therefore combined direct studies of [^{125}I]insulin binding with quantitative electron microscopic autoradiography.

Initially we studied [^{125}I]insulin binding to receptors of the well-characterized IM-9 cultured human lymphocytes and concluded (*4*):

1) Labeled insulin is initially localized on the plasma membrane (after 2 minutes of incubation at 15°C) and there is no further translocation of the labeled material.

2) At 37°C, labeled insulin is initially localized on the plasma membrane (after 2 minutes of incubation), but with continued incubation a small proportion of the labeled material moves from 350 to 750 nm from the plasma membrane (10 to 15 percent of the cell's radius).

3) Autoradiographic grains that appear 350 nm or more from the plasma membrane are not preferentially associated with intracellular organelles.

Since the liver is one of the primary targets of insulin in terms of biological action, degradation, and receptor regulation, we studied the binding of [^{125}I]-insulin to freshly isolated rat hepatocytes. We assumed that the shortest periods of incubation at the lowest temperatures most closely simulate initial binding and that subsequent steps should occur as a function of time and increasing temperature of incubation. When freshly isolated hepatocytes are incubated with $5 \times 10^{-10}M$ [^{125}I]insulin for 5 minutes at 20°C, a small proportion of the labeled hormone is bound to the cell (about 20 percent of maximum binding). When these cells are fixed, sectioned, and prepared for autoradiography, the distribution of autoradiographic grains can be determined by a quantitative analysis (*5*). In the IM-9 cultured human lymphocyte incubated at 15°C for 2 minutes, the grains are symmetrically distributed around the plasma membrane, which is consistent with the initial localization of [^{125}I]insulin on the plasma membrane (Fig. 1A). When the distance from the center of the grains to the plasma membrane in isolated hepatocytes incubated for 5 minutes at 20°C is plotted in an identical fashion a very similar pattern is seen in the lymphocyte and the hepatocyte (Fig. 1). We interpret this to mean that in both the lymphocyte and the hepatocyte, [^{125}I]insulin binding occurs initially on the plasma membrane.

To determine if there is a shift in this grain distribution as a function of in-

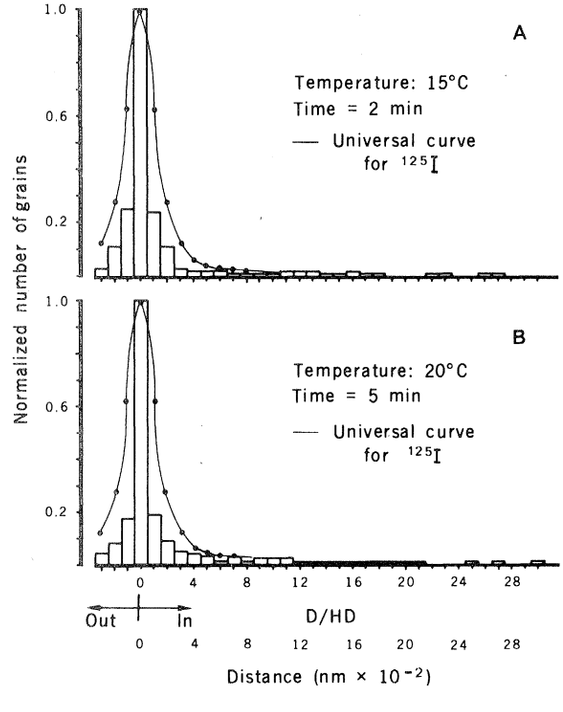

Fig. 1. Initial distribution of [^{125}I]insulin in (A) IM-9 cultured human lymphocytes and (B) isolated hepatocytes. The methods of binding, preparation for autoradiography, and analysis of data for the hepatocyte are similar to the methods used for the lymphocyte (*4*) and will be described elsewhere (*14*). Briefly, hepatocytes are isolated from 6- to 8-week-old male rats (*16*). The cells are suspended in buffer and washed by low-speed centrifugation. This procedure is repeated four times. The final suspension consists of 95 percent hepatocytes with 85 percent viability (trypan blue exclusion). Porcine monocomponent insulin was labeled with ^{125}I by a modification of the chloramine T method and purified by filtration on Sephadex G-50 (*17*). Hepatocytes (1×10^6 cells per milliliter) are incubated with $5 \times 10^{-10}M$ [^{125}I]insulin in 0.5 ml of Krebs-Ringer bicarbonate buffer (*p*H 7.7), containing 25 mg of bovine serum albumin (fraction V) per milliliter and bacitracin (0.8 mg/ml) for 5 minutes at 20°C. At the end of the incubation period 1 ml of chilled buffer is added to each tube and the tubes are centrifuged at 50*g* for 20 seconds; the supernatant is discarded and the cell pellet quickly resuspended in 1 ml of fresh chilled buffer and centrifuged for 90 seconds at 500*g*. Cell pellets are washed once more without resuspension with chilled buffer containing sucrose (100 mg/ml). Glutaraldehyde (4 percent) is added to one portion of cells, and after fixation for 4 hours at room temperature the glutaraldehyde is replaced by 0.1*M* phosphate buffer, *p*H 7.4. The second portion of cells is used to determine the amount of bound radioactivity. The glutaraldehyde-fixed cells are then dehydrated, embedded, sectioned, and coated with a thin emulsion of Ilford L4. They are then incubated for 3 to 5 weeks and developed in Microdol X (*4*). The developed grain distribution is analyzed quantitatively by the method of Salpeter *et al.* (*5*). In this analysis the normalized number of grains (vertical axis) is plotted as a function of the distance of the grain center to the plasma membrane and a histogram is constructed. The solid line represents the universal curve of ^{125}I irradiation and is derived from the distribution of ^{125}I irradiation around a defined line source (*5*). The scale designated *HD* (half distance) is a unit that describes the distance in which 50 percent of grains will appear around a defined line source. In our study 1 HD = 100 nm. This extrapolated unit does not enter further into the analysis of the data and is used here only for comparison with the universal curve.

0036-8075/78/0519-0782$00.50/0

creasing time and incubation temperature, we incubated freshly isolated hepatocytes with $5 \times 10^{-10}M$ [^{125}I]insulin at 37°C for 60 minutes. Portions of the cell suspensions were prepared for autoradiographic studies at each of the time points shown in Fig. 2A. Under these conditions, maximum binding occurred at 10 to 20 minutes and was maintained for up to 30 minutes. Nonspecific binding was less than 13 percent of the total throughout the incubation. The grain distribution for the 2-minute time point (Fig. 2B) in the lymphocytes was similar to that in hepatocytes (Fig. 1), but a small shift to the right was beginning to appear in the grain distribution in the hepatocytes. As the grain distribution for the subsequent time points at 37°C was analyzed, we found that a systematic shift of a progressively increasing number of grains occurred between 2 and 30 minutes of incubation. Thus an increasing proportion of grains appeared between 300 and 1600 nm from the plasma membrane; this effect appeared to plateau between 30 and 60 minutes (Fig. 2B).

These data indicate that after 5 minutes of incubation at 20°C the grains are localized on the plasma membrane, but with increasing time and temperature of incubation there is a progressive translocation of grains to a distance of no greater than 15 percent of the radius of the cell (cell diameter, 22 μm). At 30 minutes of incubation there is a significant shift of the grain distribution. This effect is qualitatively similar but quantitatively much greater than that observed in the cultured lymphocyte (*4*). This additional band of irradiation cannot be accounted for by potential artifacts such as damaged cells, nonspecific binding, background, or wide-angle scatter of irradiation (*4*).

To determine the nature of the cell-bound radioactivity we extracted cells at the end of each period of association and filtered the extract on Sephadex G-50 (Fig. 3). Under these circumstances, from 68 to 81 percent of the recovered radioactivity was eluted in the position of [^{125}I]insulin (Table 1). The additional radioactivity was eluted in the void volume and after the elution of the ^{125}I marker. The low-molecular-weight eluate is thought to be iodotyrosyl peptides that loosely adsorb to the column and are typical degradation products of insulin. The nature of the void volume component is unknown, but it increases with incubation time (Table 1) and occurs significantly only at 37°C. The pattern of our cell extract is remarkably similar to that of Terris and Steiner (*2*) who measured both hepatocytes and incubation media but at a somewhat lower temperature and for a shorter period of time. The void volume peak was noted by Terris and Steiner and by Kahn and Baird (*6*) in extracts of adipose cells incubated under similar conditions. Additional studies indicate that the radioactivity eluted in the region of [^{125}I]insulin is predominantly precipitable by trichloroacetic acid, adsorbs to talc, and rebinds to liver membranes (Table 2). We interpret these data to mean that the radioactivity associated with the cell under the conditions of this study maintains many of the characteristics of intact insulin and that the autoradiographic grains are predominantly derived from this radioactivity.

These data indicate that in vitro under the conditions of this study, the initial binding step of insulin to the plasma membrane of hepatocytes is followed by a progressive intracellular shift of the labeled hormone (or a product of the labeled hormone) to a limited area of the cell periphery. The reason for the apparently limited intracellular shift is unclear; however, we recently demonstrated that the intracellular grains progressively associate with lysosomes at 37°C. We have demonstrated exactly the same sequence of events for epidermal growth factor

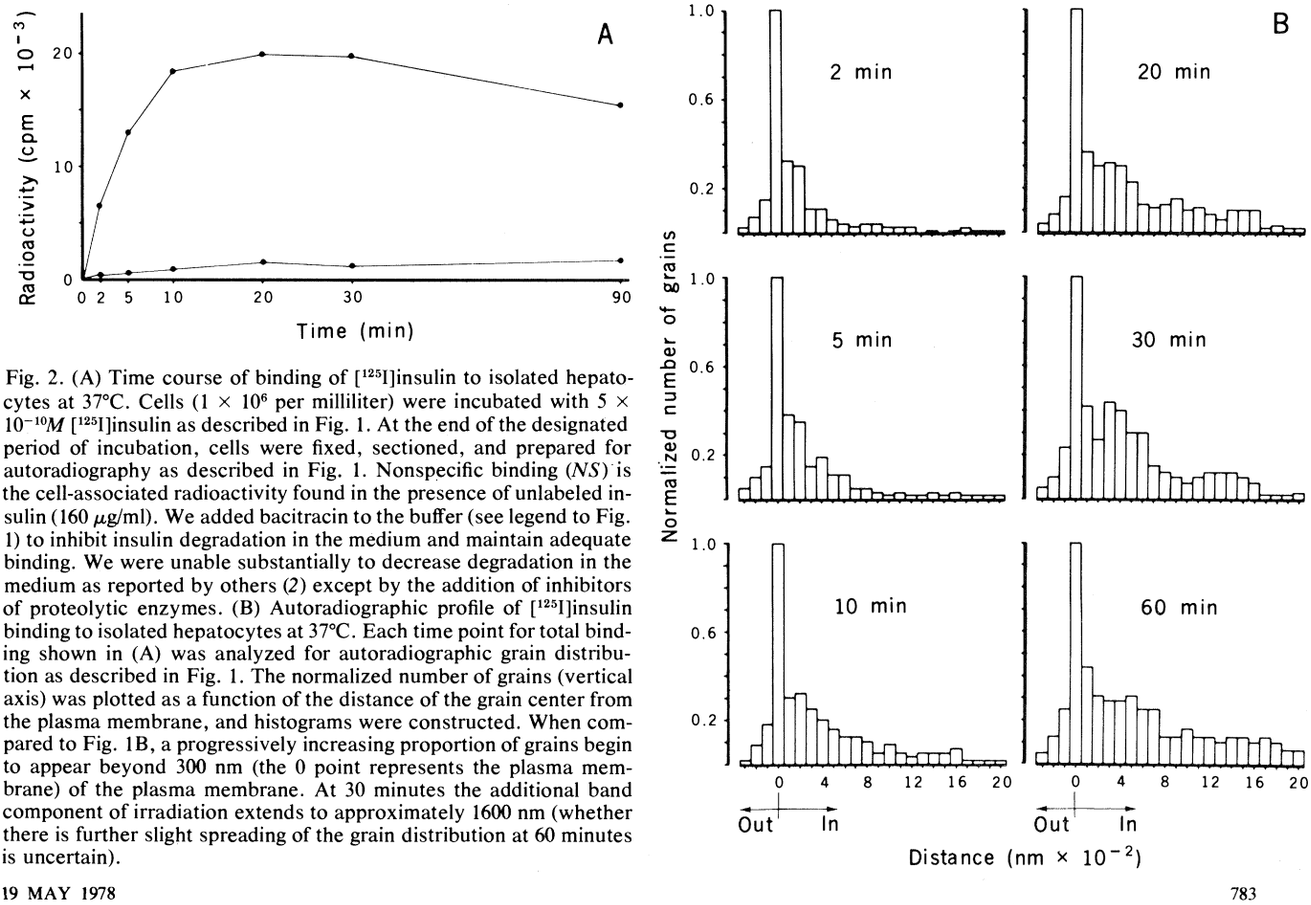

Fig. 2. (A) Time course of binding of [^{125}I]insulin to isolated hepatocytes at 37°C. Cells (1×10^6 per milliliter) were incubated with $5 \times 10^{-10}M$ [^{125}I]insulin as described in Fig. 1. At the end of the designated period of incubation, cells were fixed, sectioned, and prepared for autoradiography as described in Fig. 1. Nonspecific binding (*NS*) is the cell-associated radioactivity found in the presence of unlabeled insulin (160 μg/ml). We added bacitracin to the buffer (see legend to Fig. 1) to inhibit insulin degradation in the medium and maintain adequate binding. We were unable substantially to decrease degradation in the medium as reported by others (*2*) except by the addition of inhibitors of proteolytic enzymes. (B) Autoradiographic profile of [^{125}I]insulin binding to isolated hepatocytes at 37°C. Each time point for total binding shown in (A) was analyzed for autoradiographic grain distribution as described in Fig. 1. The normalized number of grains (vertical axis) was plotted as a function of the distance of the grain center from the plasma membrane, and histograms were constructed. When compared to Fig. 1B, a progressively increasing proportion of grains begin to appear beyond 300 nm (the 0 point represents the plasma membrane) of the plasma membrane. At 30 minutes the additional band component of irradiation extends to approximately 1600 nm (whether there is further slight spreading of the grain distribution at 60 minutes is uncertain).

binding to human fibroblasts (*7*) (that is, initial plasma membrane binding followed by internalization and lysosomal association) as we have for insulin binding to isolated hepatocytes. These findings for epidermal growth factor confirm the predictions of Carpenter and Cohen (*8*) made on the basis of their binding studies. To further corroborate our quantitative autoradiographic method we studied the binding of low-density lipoprotein in human fibroblasts and found, as previously demonstrated by binding studies and ferritin conjugates (*9*), that binding at 4°C is restricted to the plasma membrane but at 37°C the material is internalized and associates with lysosomes.

Terris and Steiner (*2*) have described a receptor-linked form of insulin degradation and have suggested that this may be an intracellular process. If this degradative process has physiological relevance then our data would provide a mechanism by which the process could occur.

The only known mechanism for internalization of a macromolecule is endocytosis. If labeled insulin is internalized by the process of adsorptive pinocytosis, it is likely that the hormone-receptor complex is internalized by endocytosis. Typically, membrane vesicles that have undergone endocytosis associate with lysosomes (*10*). The binding of a ligand to its specific receptor followed by endocytosis of the complex would provide a specific mechanism for ligand-induced receptor loss. Insulin-induced receptor loss has been demonstrated in vivo in rodent hepatocytes and liver membranes as well as many other tissues of the rodent and in peripheral monocytes and adipocytes in man (*3*, *11*).

Insulin has no effect on the membrane transport of carbohydrate in liver; its main effect appears to be related to the regulation of intracellular enzymes. The hepatocytes used for these experiments are metabolically active in response to hormones (*12*). In a similar preparation of cells and after a similar time of incubation, glycogen synthetase activation by insulin has been demonstrated (*13*).

It is important to emphasize that the associations we make between the findings of this study and the actions of insulin are speculative, but it is possible that the binding of insulin to its specific receptor followed by ligand-induced endocytosis provides a link between several apparently diverse functions of insulin (*14*).

Table 1. Percentage of radioactivity recovered by Sephadex G-50 gel filtration from cell extracts obtained during association of [^{125}I]insulin with hepatocytes. The methods used are described in Fig. 3.

Peak	Time of association at 37°C (minutes)					
	2	5	10	20	30	60
I	4	7	4	7	9	15
II	80	68	81	72	72	70
III	4	10	5	8	3	6

Table 2. Percentage of cell-associated radioactivity precipitated by 10 percent trichloroacetic acid and adsorbed by talc. The method used is described in (*15*). Peak I radioactivity was not evaluated because of the low counts. In addition, in several extracts we tested the rebinding of peak II radioactivity to liver membranes and found that the lyophilized peak II extract bound from 60 to 100 percent of the radioactivity as well as fresh labeled insulin exposed to the same solvent and lyophilization conditions.

Treatment of cells	Time of association at 37°C (minutes)							
	5		20		30		60	
	II	III	II	III	II	III	II	III
Precipitated by trichloroacetic acid	99	35	93	33	84	49	83	51
Adsorbed by talc	82	40	81	38	82	39	82	44

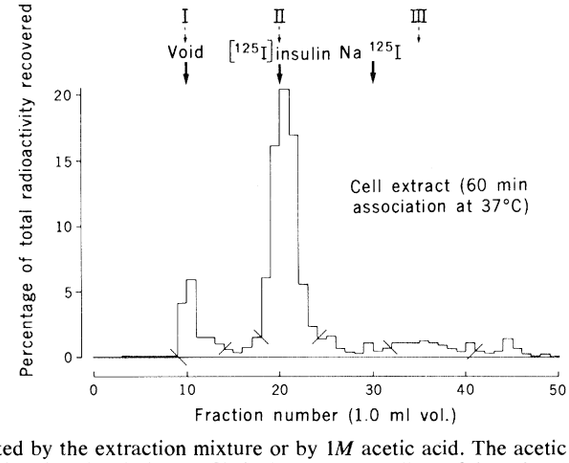

Fig. 3. Sephadex G-50 gel filtration elution profile of extract of cell-associated radioactivity. At the end of each time point of incubation (shown in Fig. 2B) cells are centrifuged and the pellet washed with buffer. The cell pellet is then extracted with a mixture of 0.1 percent Triton X-100, 3*M* acetic acid, and 6*M* urea and the mixture centrifuged in a Beckman microfuge at 12,000*g* for 5 minutes. Under these conditions, 95 to 98 percent of the total cellular radioactivity is found in the supernatant. The extract is then applied to a G-50 (fine) column (0.9 by 50 cm) which is either equilibrated in and eluted by the extraction mixture or by 1*M* acetic acid. The acetic acid is used to permit lyophilization, but the elution profile is the same regardless of the solvent used, and total radioactivity recovered from the column was 80 to 85 percent of that applied. The peak elution volume of the void, [^{125}I]insulin, and Na^{125}I are shown at the top and the slashes designate the peaks referred to as I, II, and III. The percentage of radioactivity eluted in each of these peaks is shown in Table 1; the percentage of trichloroacetic acid precipitability and talc adsorption for the lyophilized extract of peaks II and III are shown in Table 2. The example shown in this figure is taken from the 60-minute time point in Table 1.

P. GORDEN
J.-L. CARPENTIER
Institute of Histology and Embryology, University of Geneva Medical School, Geneva, Switzerland
P. FREYCHET
A. LECAM
Institut National de la Santé et de la Recherche Médicale, Faculté de Médecine (Pasteur), Nice, France
L. ORCI
Institute of Histology and Embryology, University of Geneva Medical School

References and Notes

1. J. Roth, *Metabolism* **22**, 1059 (1973).
2. S. Terris and D. F. Steiner, *J. Biol. Chem.* **250**, 8389 (1975).
3. R. S. Bar, P. Gorden, J. Roth, C. R. Kahn, P. De Meyts, *J. Clin. Invest.* **58**, 1123 (1976).
4. J.-L. Carpentier, P. Gorden, M. Amherdt, E. Van Obberghen, C. R. Kahn, L. Orci, *ibid.*, in press.
5. M. M. Salpeter, H. C. Fertuck, E. E. Salpeter, *J. Cell Biol.* **72**, 161 (1977); M. M. Salpeter and F. A. McHenry, in *Advanced Techniques in Biological Electron Microscopy*, J. K. Koehler, Ed. (Springer-Verlag, Berlin 1973), p. 113; M. M. Salpeter and L. Bachman, in *Principles and Techniques of Electron Microscopy. Biological Applications*, M. A. Hayat, Ed. (Van Nostrand Reinhold, New York, 1972), p. 220.
6. C. R. Kahn and K. L. Baird, *Diabetes* **1** (Suppl.), 354 (1977).
7. P. Gorden, J.-L. Carpentier, S. Cohen, L. Orci, Proceedings of the 16th Endocrine Society, Miami, Fla., in press.
8. G. Carpenter and S. Cohen, *J. Cell Biol.* **71**, 159 (1976).
9. J.-L. Carpentier, P. Gorden, L. Orci, M. S. Brown, J. L. Goldstein, in preparation; R. G. W. Anderson, M. S. Brown, J. L. Goldstein, *Cell* **10**, 351 (1977).
10. A. C. Silverstein, R. M. Steinman, Z. A. Cohn, *Annu. Rev. Biochem.* **46**, 669 (1977).
11. C. R. Kahn, D. M. Neville, Jr., P. Gorden, P.

Freychet, J. Roth, *Biochem. Biophys. Res. Commun.* **48**, 135 (1972); J. M. Olefsky, *Diabetes* **25**, 1154 (1976).
12. A. Le Cam and P. Freychet, *Biochem. Biophys. Res. Commun.* **72**, 893 (1976); P. Freychet and A. Le Cam, *Ciba Found. Symp.*, in press; A. Le Cam and P. Freychet, *Mol. Cell. Endocrinol.*, in press; ———, in preparation.
13. L. A. Witters, L. Alberico, J. Avruch, *Biochem. Biophys. Res. Commun.* **69**, 987 (1976).
14. J.-L. Carpentier, P. Gorden, A. Le Cam, P. Freychet, L. Orci, *Diabetologia* **13**, 386 (1977); ———, in preparation; P. Gorden, J.-L. Carpentier, P. Freychet, A. Le Cam, L. Orci, *Diabetes*, in press (abstract).
15. P. Freychet, C. R. Kahn, J. Roth, D. M. Neville, Jr., *J. Biol. Chem.* **247**, 3953 (1972).
16. A. Le Cam *et al.*, *Exp. Cell Res.* **98**, 382 (1976).
17. P. Freychet, in *Methods in Receptor Research*, M. Blecher, Ed. (Dekker, New York, 1976), p. 385.
18. Supported by grant 3.120.77 from the Swiss National Science Foundation, and by grant 77.7.0247 from the Délégation Générale à la Recherche Scientifique et Technique (France). This work was performed while P.G. was a visiting professor at the Institute of Histology and Embryology in Geneva.

13 October 1977; revised 8 March 1978

Another Flame Retardant, Tris-(1,3-Dichloro-2-Propyl)-Phosphate, and Its Expected Metabolites Are Mutagens

Abstract. *A flame retardant used in children's sleepwear, tris-(1,3-dichloro-2-propyl)phosphate (Fyrol FR2) is a mutagen in the* Salmonella*-mammalian tissue homogenate test after it has been activated by mouse or rat liver homogenate. The expected enzymatic hydrolysis product, 1,3-dichloro-2-propanol, is similarly a mutagen after activation by liver homogenate. A proposed metabolite of the flame retardant, 1,3-dichloro-2-propanone, is a potent mutagen in the absence of such activation. A flame retardant with similar structure, tris-(2,3-dibromopropyl)phosphate (tris-BP), was shown previously to be a mutagen, to cause sterility in animals, to be a carcinogen, and to be absorbed through human skin. These and other flame retardants have characteristic nuclear magnetic resonance spectra that can be used to determine which flame retardant is present in commercially purchased sleepwear. Sleepwear treated with tris-BP, Fyrol FR2, and other chemical additives was being sold in late 1977.*

In 1972 the United States established flammability standards for children's sleepwear. To comply with these standards, manufacturers began to use chemical additives (usually organic halogens or phosphate esters or both) to confer flame-resistant properties on the fabric. The most widely used of these flame retardants was the mutagen and carcinogen, tris-(2,3-dibromopropyl)phosphate (tris-BP) (*1*–*5*).

Although tris-BP is no longer being used to treat children's sleepwear, in late 1977 many millions of treated garments were still in storage (*6*) and some were still being sold. Other similar flame retardants are being used as replacements for tris-BP. We report here the finding that one of them which is structurally similar to tris-BP, namely tris-(1,3-dichloro-2-propyl)phosphate (Fyrol FR2) (*7*), and two of its expected metabolites, 1,3-dichloro-2-propanol and 1,3-dichloro-2-propanone, are mutagens (*8*).

In 1975, 6 to 10 million pounds (1 kilogram = 2.2 pounds) of Fyrol FR2 were produced in the United States (*9*). Although we have not been able to obtain production figures indicating what fraction of this amount was used to treat children's sleepwear, we have analyzed a selection of infants' pajamas in order to see whether Fyrol FR2 has replaced tris-BP as a flame retardant for polyester. Fyrol FR2 is used to treat garments made of polyester; tris-BP was used to treat both polyester and polyester blended with acetate or triacetate.

Children's pajamas (50 pairs) made of polyester and polyester blends (sizes 0 to 6X) were purchased in several states during the period from June through October 1977. A fabric sample from each garment was extracted in acetone and the resulting extracts analyzed by nuclear magnetic resonance (NMR). Typical NMR spectra of sleepwear extracts and flame retardants are shown in Fig. 1. Seventeen of the 50 pajamas, all of the polyester blend fabrics, were found to have been treated with tris-BP and nine of the polyester fabrics had been treated with Fyrol FR2, based on comparison of the NMR spectra of the extracts with those of the pure chemicals. Two of the other pajamas made of polyester had been treated with Mobil Antiblaze 19, a mixture of cyclic phosphate esters (*8*), and the remaining 22 pajamas showed no identifiable NMR spectrum. In addition to the NMR spectra attributable to the flame retardants, the sleepwear showed other peaks, mainly in the alkane region (< 3 parts per million), which are thought to be due to other chemical additives in the fabrics.

Prior to this work, Fyrol FR2 was negative in a mutagenicity test (*1*), in which polychlorinated biphenyl (PCB)–induced rat liver homogenates were used (*10*). However, a more thorough examination of Fyrol FR2 and its expected metabolites was undertaken because (i) Fyrol FR2 is very similar in structure to tris-BP; (ii) the structure of one expected metabolite, 1,3-dichloro-2-propanone, suggested it would be a potent alkylating agent and therefore a mutagen or carcinogen; and (iii) the structure of another expected metabolite, 1,3-dichloro-2-propanol, suggested it would be a mutagen after metabolic activation.

As illustrated in Fig. 2, Fyrol FR2 and dichloropropanol were weakly mutagenic on *Salmonella typhimurium* strain TA100 in the presence of phenobarbital-induced mouse liver homogenate. Dichloropropanone was strongly mutagenic on TA100 and required no activation. Each of six independent experiments with Fyrol FR2 with phenobarbital-induced mouse liver homogenate showed a dose response for mutagenicity. A repeatable dose response was also obtained in two experiments in the presence of PCB-induced mouse liver homogenate and in three experiments with phenobarbital-induced rat liver homogenate. The weakest response occurred with PCB-induced rat liver homogenate (*11*). Recently, a coded experiment on the mutagenicity of tris-BP and two samples of 96 percent Fyrol FR2 (supplied by Stauffer) confirmed these results. The mutagenicity of Fyrol FR2 was further confirmed in another laboratory in three tests in which PCB-induced mouse liver homogenate was used and in four tests in which PCB-induced hamster liver homogenate was used for activation (*12, 13*).

Metabolic transformations of Fyrol FR2 to mutagens are proposed in Fig. 3 by analogy with the known metabolism of other related phosphotriesters (*14*). Oxidative *O*-dealkylation of Fyrol FR2 would be expected to produce 1,3-dichloro-2-propanone, which we show here to be a powerful direct-acting mutagen. A precedent for this would be the transformation of the pesticide chlorfenvinphos, which is oxidatively *O*-deethylated by liver microsomes in the presence of reduced nicotinamide adenine dinucleotide phosphate (NADPH) and oxygen (*15*). Diisopropyl-1-naphthyl phosphate has been shown to undergo a similar dealkylation (*15*). Cleavage of the phosphate triester bonds in Fyrol FR2 by hydrolases in the cell would yield dichloropropanol, which we show here to be a mutagen in the presence of liver homogenate. Enzymes hydrolyzing phosphotriesters are found in many mammalian tissues (*14*). The glutathione *S*-transferases (*14*) would be expected to form glutathione adducts of Fyrol FR2, di-

0036-8075/78/0519-0785$00.50/0